ISBN: 978-3-95450-132-8 doi:10.18429/JACoW-IPAC2014-TUYA01

FIRST EXPERIENCE WITH ELECTRON LENSES FOR BEAM-BEAM COMPENSATION IN RHIC*

W. Fischer†, X. Gu, S.M. White, Z. Altinbas, D. Bruno, M. Costanzo, J. Hock, A. Jain, Y. Luo, C. Mi, R. Michnoff, T.A. Miller, A.I. Pikin, T. Samms, Y. Tan, R. Than, P. Thieberger
Brookhaven National Laboratory, Upton, New York, USA

Abstract

The head-on beam-beam interaction is the dominant luminosity limiting effect in polarized proton operation in RHIC. To mitigate this effect an electron lens was installed in each of the two RHIC rings. We summarize the hardware and electron beam commissioning results to date, and report on the first experience with the electron-hadron beam interaction. In 2014 to date, RHIC has operated with gold beams only. In this case the luminosity is not limited by head-on beam-beam interactions and compensation is not necessary. The goals of this years commissioning efforts are a test of all instrumentation; the demonstration of electron and gold beam overlap; the demonstration of electron beam parameters that are sufficiently stable to have no negative impact on the gold beam lifetime; and the measurement of the tune footprint compression from the beam overlap. With these demonstrations, and a lattice with a phase advance that has a multiple of 180 degrees between the beam-beam interaction and electron lens locations, head-on beam-beam compensation can be applied in the following year with proton beams.

INTRODUCTION

In RHIC there are 2 head-on (Interaction Points IP6 and IP8) and 4 long-range beam-beam interactions with large separation (10 mm) between the beams. The polarized proton luminosity is limited by head-on effects [1]. Two electron lenses are installed near IP10 in a region common to both RHIC beams (Fig. 1) to compensate for one of the two head-on collisions. Together with an increase in the bunch intensity [2] an increase in the luminosity is planned by up to a factor of two.

The design of the RHIC electron lenses was based on the experience with the Tevatron lenses [3–6] and the BNL Electron Beam Ion Source (EBIS) [7]. The design was also guided by extensive beam-beam simulations [8]. Design and construction progress were reported previously (Refs. [9, 10] and references therein). Both lenses are now installed and commissioning with Au beams began in 2014. The lifetime of colliding Au beams is not limited by beam-beam effects, and with cooling [11] losses are dominated by burn-off. With Au beams the functionality of the electron lens can be tested by observing phenomena such as effects on orbit and tune, beam loss rates, emittance growth, and the stability of the hadron beams. The cooled Au beams allow for quench training and emittance growth tests during physics stores. The main parameters for the 2014 Au run and the 2015 p run are shown in Tab. 1. The 2014 Au run is not yet complete and more tests than reported here are planned. There is also a short h+Au (helium-3 on gold) run planned [12]. The 2015 p run will be the first during which head-on beam-beam compensation can be applied.

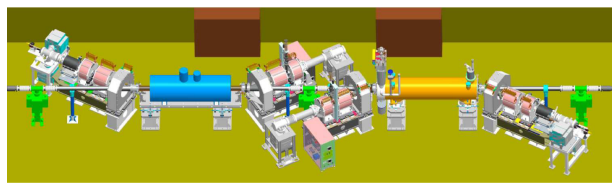

Figure 1: Layout of the two electron lenses in IR10. In each lens three beams are present, the two hadron beams and the electron beam acting on one of the hadron beams. The two hadron beams are vertically separated.

Table 1: RHIC and electron lens parameters for the 2014 commissioning run with Au beams, and the planned 2015 operation with p beams. In both cases numbers are shown for the maximum instantaneous luminosity, which for Au is reached after about 1 h due to cooling.

quantity	unit	value	
		2014 Au	2015 p
hadron beam parameters			
total energy E	GeV/nucleon	100	100
bunch intensity N_b	10^9	1.6	250
$\beta^*_{x,y}$ at IP6, IP8 (Au+Au, p+p)	m	0.7	0.85
$\beta^*_{x,y}$ at IP10 (Au+e, p+e)	m	10.0	20.0
rms emittance ϵ_n	μm	1.0	2.5
rms beam size at IP6, IP8 σ^*_p	μm	80	140
rms beam size at IP10 σ^*_p	μm	300	685
rms bunch length σ_s	m	0.30	0.60
hourglass factor F	...	0.7	0.85
beam-beam parameter ξ/IP	...	-0.006	-0.012
number of beam-beam IPs	...	— 2+1* —	
electron lens parameters			
distance of center from IP	m	— 3.3 —	
effective length L_e	m	— 2.1 —	
kinetic energy E_e	keV	10	9.5
current I_e	A	1.0	0.9
beam-beam parameter	...	$+0.005$	$+0.012$
main solenoid field	T	3, 4	5
rms beam size σ_e	μm	500, 425	685

*One head-on collision in IP6 and IP8 each, and a head-on collision at the electron lens in IP10.

* Work supported by Brookhaven Science Associates, LLC under Contract No. DE-AC02-98CH10886 with the U.S. Department of Energy.
† Wolfram.Fischer@bnl.gov

ISBN: 978-3-95450-132-8 doi:10.18429/JACoW-IPAC2014-TUYA01

HARDWARE COMMISSIONING

The superconducting solenoids were designed for a field of 6 T and reached this field in the vertical test. In one of the magnets, installed in Blue, the innermost of 11 double layers was grounded to reach the 6 T field, and the currents in the two magnets are therefore different for the same field. In the summer of 2013 both magnets were tested horizontally in the RHIC tunnel and reached 5 T. The magnets were not trained further since the helium for cooling was supplied by dewars and training quenches constituted a considerable cost. In 2014, with helium supplied by the RHIC refrigerator, the Yellow solenoid has reached 6.0 T, and the Blue solenoid 4.4 T so far with three training quenches. With cooled Au beams it is possible to train the magnets during a physics store. Since the two superconducting main solenoids are of opposite polarity and are always operated concurrently, the disturbances are small enough. A small He leak into the insulating vacuum developed in the Yellow solenoid, and required the installation of a small turbo pump. Without the pump the pressure would increase over several weeks to 10^{-3} Torr, and the additional heat load would prevent operation of the magnet.

Both solenoids have 2.5 T fringe field (FF) coils at both ends that ensure a minimum solenoid field of 0.3 T between the superconducting and warm solenoids for all operating conditions. Initially the FF coils quenched at the leads below their operating current due to insufficient cooling. An increase in the helium flow rate provided sufficient cooling but led to ice ball formation, which was remedied by heating and flowing dry air over the leads.

The straightness of the solenoid field lines has tight tolerances (± 50 μm over a range of ± 800 mm) to ensure good overlap of the hadron and electron beam. Five horizontal and five vertical dipole correctors are installed in both lenses to straighten the field lines. A measurement system was built based on a magnetic needle and mirror which are pulled through the solenoid [13]. Figure 2 shows the measurement results for the vertical plane of magnet no. 2, installed in the Yellow lens. Both solenoids met the straightness tolerances in both planes at 2, 3, and 4 T, and no further correction is necessary.

The warm solenoids that transport the electron beam into and out of the interaction region (Fig. 1) change the vertical orbit rms by several millimeters at injection. These effects are compensated with the orbit feedback [14].

The lenses can be operated in pulsed mode (beam on for a fraction of a turn) and DC mode. Both gun and collector needed some conditioning to have a good vacuum in the interaction region. A drift tube system is installed in both lenses [10] to extract ions that accumulate in the interaction region due to residual gas ionization and the potential created by a DC electron beam. After bake-out it was found that only three of the five drift tubes in the Blue lens hold high voltage, and none in the Yellow lens.

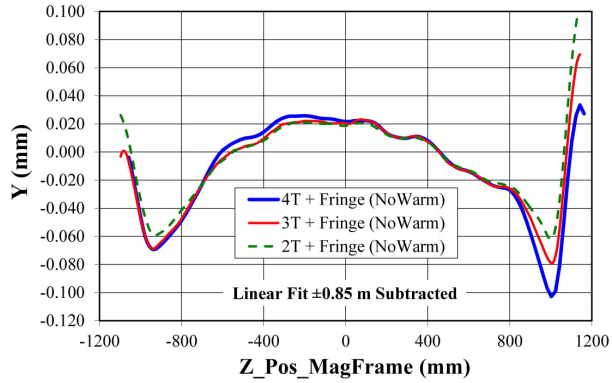

Figure 2: Vertical solenoid field straightness measurement in the Yellow lens magnet. The rms beam size at 255 GeV is as small as 300 μm.

ELECTRON BEAM COMMISSIONING

The goals of the electron beam commissioning were to demonstrate the required electron beam current in pulsed and DC mode, and to measure the transverse profiles that need to be Gaussian.

After initial gun and collector conditioning, the electron beam current was slowly increased, and the lenses operated concurrently with Au beam stores. For this a pulsed electron beam was turned on overlapping the abort gap. During the ramp up of the electron beam current there were two instances where a large pressure spike occurred, leading to a doubling of the Au beam emittances.

Both electron lenses ran at a maximum pulsed current of 1 A for 5 h concurrent with a RHIC store (in the abort gap), and with 1 A DC current without Au beams. A DC beam test during physics stores would produce a tune shift of $+0.006$ in both planes (Tab. 1).

A Gaussian electron beam profile is essential for the correction of the nonlinear beam-beam effects. To verify the Gaussian profile the electron lenses have two transverse profile measurement systems: a YAG screen and a pinhole detector over which the electron beam is scanned. Figure 3 shows the vertical profile of the Yellow electron beam measured with the YAG crystal. A flattening of the top is visible (also in the horizontal plane), which can be either due to saturation or an actual reduction in the current in the center where the density is the highest. Simulations indicate that the measured deviations from the Gaussian profile are acceptable.

COMMISSIONING WITH AU BEAMS

In 2014 to date, RHIC operated only with Au beams [12]. The colliding Au beams are cooled [11], and almost all beam losses are from burn-off. The cooling time is about 1 h (as is the IBS growth time without cooling). The beam-beam effects with Au beams are small and compensation is not necessary. However, the effect of the electron beam on orbit and tune can be tested, and emittance growth and beam loss studied. Commissioning with

ISBN: 978-3-95450-132-8 doi:10.18429/JACoW-IPAC2014-TUYA01

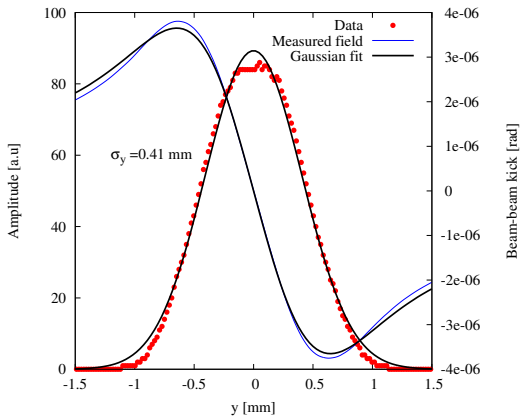

Figure 3: Vertical profile measured with the YAG crystal and Gaussian fit to the data. The beam-beam kick is calculated for the measured field and the Gaussian fit.

Au beams was done with dedicated time (4 h every other week), and parasitically during physics stores. In the latter mode either short electron pulses were affecting the last two bunches of the bunch train, or a DC electron beam affecting all of the Au bunches.

Orbit and tune response. As a first test the effect of the electron beam on the orbit and tune of the Au beam was measured at injection and store with separate transverse scans of the Au and electron beams. This was also the first method to align the beams. It would be cumbersome for routine alignment and was quickly replaced by an automatic procedure using backscattered electrons (see below). Figure 4 shows the measured horizontal and vertical tunes as a function of the vertical separation.

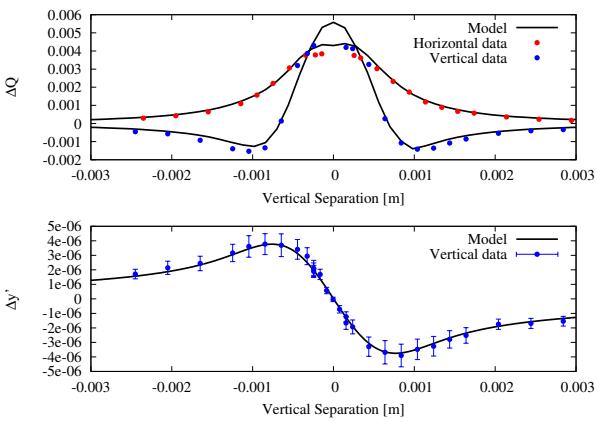

Figure 4: Change of gold beam orbit (top) and tunes (bottom) in response to a vertical displacement of the Yellow beam at store.

Beam Transfer Functions. Transverse Beam Transfer Function (BTF) measurements are a routine way of measuring tunes and assessing tune spread. Although the incoherent tune distribution in both planes cannot be uniquely reconstructed from BTF measurements [15] it is still possible to obtain information on tunes, tune distributions and coherent modes from BTFs. Figure 5 shows three BTF measurements with different electron beam currents. With increasing current the tunes are shifted upwards as expected and coherent modes emerge.

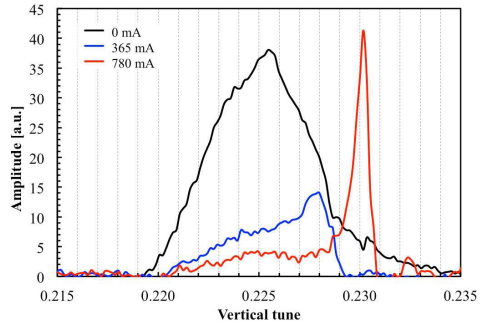

Figure 5: Tune distributions derived from BTF measurements of all bunches in the case of 0 mA, and of the last two bunches for 365 and 780 mA. With the electron lens coherent modes are emerging.

Transverse alignment. Each electron lens has a dual plane BPM at each end. These BPMs see both hadron beams and the electron beam. The rise and fall time of a pulsed electron beam is an order of magnitude longer than the rise and fall time of the bunched hadron beam. The BPMs were used to bring the electron and Au beams close for the initial alignment.

A fast and reliable alignment of the two beams has been implemented with a novel detector based on measuring backscattered electrons [16]. After a short commissioning period the new detector gave reliable signals, with counting rates ranging over six orders of magnitude. Backscattered electrons could already be detected by the electron beam interacting with the residual gas (the signal responds to pressure changes), and the Au beam halo. The signal was used in an application to maximize the overlap region through automatic position and angle scans (Fig. 6), the same application that also maximizes the luminosity of the STAR and PHENIX experiments.

Beam loss and emittance growth. With Au beams in physics operation the electron beam is about twice as large as the Au beam (Tab. 1). The electron lens therefore introduces predominantly a tune shift, which after correction, should lead to no additional beam loss or emittance growth. Since the electron lens will introduce some nonlinearities and the Au lattice is not optimized for beam-beam compensation, small increases in loss rates and emittances may be possible. The cooling time of about 1 h sets the resolution for the detection of additional emittance growth. Un-cooled beams provide the same resolution since the additional emittance growth needs to be distinguished from the IBS growth time, also of order 1 h.

Initial emittance growth tests were made with electron beam pulses that covered only 2 bunches to separate out

ISBN: 978-3-95450-132-8 doi:10.18429/JACoW-IPAC2014-TUYA01

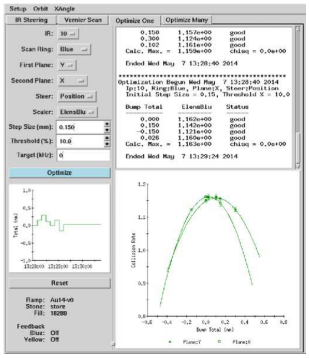

Figure 6: Application for the automatic transverse alignment of hadron and electron beam by maximizing the number of backscattered electrons.

any effects arising from ion accumulation in the lenses. Conditions could be setup so that no additional beam loss or emittance growth was observed up to 500 mA electron current.

The main operating mode, however will be DC. Figure 7 shows a test in which the Blue lens electron beam current was successively increased to 800 mA, with the electron lens in Yellow off (to have loss rates and emittances for comparison). Throughout the current increase, the Blue tunes were reduced by up to $(-0.004, -0.004)$ to compensate for the additional focusing from the electron lens. The Blue emittance cooled down as fast as the Yellow emittance, and the Blue loss rate did not exceed the Yellow loss rate by more than 1%/h after tune correction. For this experiment a fill pattern was prepared with which all bunches have two collisions, and the Au and electron beams were aligned in both position and angle. The spike in the loss rate at 13:55 and the Blue emittance increase at the same time (Fig. 7) were caused by a vacuum spike when the electron beam current was raised beyond 800 mA.

With the DC beam operation it is possible that the ion accumulation in the lens leads to emittance growth since ions, created through residual gas ionization by the hadron and electron beams, are held in the transverse potential of the electron beam. Clearing electrodes are installed for the longitudinal extraction of ions through an electrostatic field. However, not all clearing electrode held voltage. The test shown in Figs. 7 and 8 were done with the three available drift tubes initially on and no clear correlation of emittance growth to bunch number is discernible. This is also the case when the the drift tubes were turned off (Fig. 8).

Instabilities. With large beam-beam parameters and electron currents, instabilities can occur since the electron beam creates a wakefield for the hadron beam. A simplified low field threshold for the instability is [17]

$$B_{th} = \frac{1.3 e N_b \xi_{el}}{r^2 \sqrt{\Delta Q Q_s}} \qquad (1)$$

where B_{th} is the main solenoid low field threshold field, N_b the proton bunch intensity, ξ_{el} the electron lens beam-beam parameter, r the proton and electron beam radii in

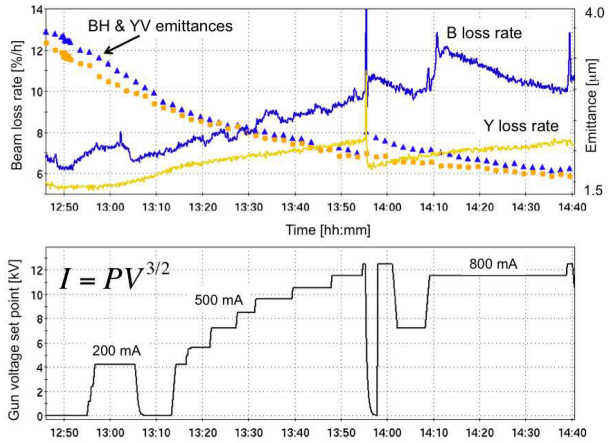

Figure 7: Blue and Yellow emittances and beam loss rates (top) as a function of the Blue electron lens gun anode voltage (bottom). The Blue tunes are readjusted by up to $(-0.004, -0.004)$ with increasing electron current (fill 18338).

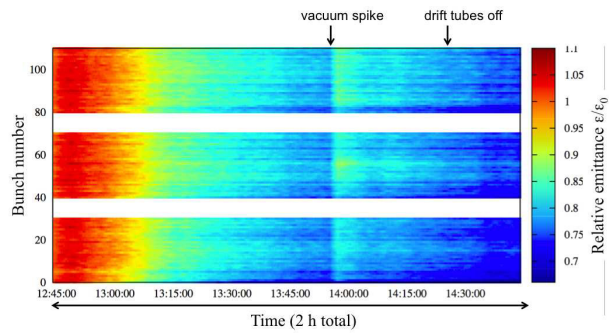

Figure 8: Blue relative emittance as a function of time and bunch number (also fill 18338, see Fig. 7). No dependence on the bunch number is visible.

the lens (assumed to be the same), ΔQ the split between the proton transverse tunes, and Q_s the synchrotron tune. Simulations show an instability for the highest beam-beam parameters considered in p operation [18]. A test was made with Au beam, in which the solenoid main field was lowered to 1.5 T, which still allowed for electron beam propagation through the lens, and for which simulations also showed unstable behavior. No instability was observed in the experiment.

PREPARATION FOR 2015

In 2015 RHIC will operate with polarized protons at 100 GeV beam energy, which presents the first opportunity for the electron lenses to compensate the head-on beam-beam effects. No operation at the maximum beam energy of 255 GeV is planned. This allows the use of a larger cathode (radius of 7.5 mm instead of 4.1 mm) in conjunction with a 5 T solenoid field to match the beam sizes. The higher solenoid field increases the instability threshold (Eq. (1)).

In addition, one of the authors (SMW) developed two

ISBN: 978-3-95450-132-8 doi:10.18429/JACoW-IPAC2014-TUYA01

new lattice versions, with the preferred version based on the ATS optics [19]. The new lattice has the correct phase advance between IP8 and the electron lenses, a larger β-functions at the electron lens (see Tab. 1), and a small nonlinear chromaticity. With the new lattice the dynamic aperture with half beam-beam compensation is independent of the bunch intensity up to a value of 3×10^{11} (Fig. 9).

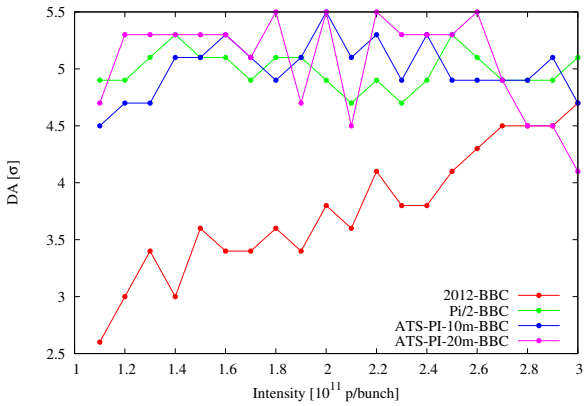

Figure 9: Dynamic aperture as a function of proton bunch intensity for different Blue lattices.

SUMMARY

The RHIC electron lenses for head-on beam-beam compensation are installed, and have been commissioned with gold beams. The magnet structure is operational with a main solenoid field of 4.4 T in one and 6.0 T in the other ring, and deviations of the solenoidal field of no more than ± 50 μm from a straight line over a range of ± 800 mm. Electron beam currents of up to 1 A have been demonstrated in pulsed and DC mode, and the transverse profile measured to be close to Gaussian.

The following instrumentation has been commissioned: (i) BPMs for both electron and hadron beam, (ii) electron beam halo detector at the collector entrance, (iii) electron beam profile measurements with both YAG crystals and a pin hole detector, and (iv) beam overlap detector based on backscattered electrons. In 2014 to date, beam commissioning was only possible with Au beams. These are stochastically cooled and beam losses are predominately from burn-off, not from beam-beam interactions. With gold beams the effect of the electron lenses on orbit and tune were measured and found to be as expected. Pulsed and DC operation did not show any additional emittance growth (with a growth time resolution of 1 h).

For the 2015 polarized proton operation the following changes are planned: (i) A larger gun (7.5 mm radius vs. 4.1 mm) to allow for a larger electron beam at high solenoid field, (ii) modifications on the collector side to accommodate the larger electron beam, (iii) a repair of the drift tube system, (iv) a new ATS proton lattice with a large β-functions at the location of the electron lens (20 m vs. 10 m), the correct phase advance to the nearest proton-proton interaction, and a small nonlinear chromaticity, (v) transverse dampers in both rings, (vi) upgrades to the abort system to allow for higher total intensity.

ACKNOWLEDGMENTS

We are thankful to V. Shiltsev, A. Valishev, and G. Stancari, FNAL, who generously shared their experience with the Tevatron electron lenses; F. Zimmermann and T. Pieloni, CERN, and P. Görgen, TU Darmstadt, for discussions of beam-beam effects and BTFs. We are grateful to all groups of the BNL Collider-Accelerator Department and the BNL Superconducting Magnet Division for their support in the design, construction, installation and commissioning of the RHIC electron lenses, and in particular to M. Bai, A.K. Drees, B. Frak, D.M. Gassner, A. Marusic, M. Mapes, K. Mernick, C. Montag, M. Minty, G. Robert-Demolaize, C. Theisen, J. Tuozzolo, and W. Zhang. We are especially thankful to the STAR and PHENIX experiments that accommodated commissioning during physics stores.

REFERENCES

[1] V. Schoefer et al., IPAC 2012, New Orleans, Louisiana, USA, pp. 184-186 (2012).
[2] A. Zelenski, "OPPIS with fast atomic beam source" presentation 2011 Particle Accelerator Conference, New York, USA (2011).
[3] V. Shiltsev, V. Danilov, D. Finley, and A. Sery, Phys. Rev. ST Accel. Beams 2, 071001 (1999).
[4] V. Shiltsev et al., Phys. Rev. Lett. 99, 244801 (2007).
[5] V. Shiltsev, et al. Phys. Rev. ST Accel. Beams 11, 103501 (2008).
[6] G. Stancari et al., Phys. Rev. Lett. 107, 084802 (2011).
[7] J. Alessi (editor), "Electron Beam Ion Source Pre-Injector Project (EBIS), Conceptual Design Report", BNL-73700-2005-IR (2005).
[8] Y. Luo, W. Fischer, N.P. Abreu, A. Pikin, and G. Robert-Demolaize, Phys. Rev. ST Accel. Beams 15, 051004 (2012).
[9] X. Gu et al., Nucl. Instrum. and Methods A 743, pp. 56-67 (2014).
[10] W. Fischer et al, ICFA Mini-Workshop on Beam-Beam Effects in Hadron Colliders (BB3013), CERN (2013).
[11] M. Blaskiewicz, J.M. Brennan, and K. Mernick, Phys. Rev. Lett. 105, 094801 (2010)
[12] G. Robert-Demolaize et al., TUPRO032, these proceedings.
[13] A. Jain, 17^{th} International Magnetic Measurement Workshop, IMMW17, Barcelona, Spain (2011). immw17.cells.es/presenstations/Tue10-IMMW17-AJain.pdf
[14] M. Minty et al. PAC 2011, pp 1394-1398 (2011).
[15] P. Görgen, O. Boine-Frankenheim, and W. Fischer, ICFA Mini-Workshop on Beam-Beam Effects in Hadron Colliders (BB3013), CERN (2013); TUPRO032, these proceedings.
[16] P. Thieberger et al., BIW12, Newport News, VA (2012).
[17] A. Burov, V. Danilov, and V. Shiltsev, Phys. Rev. E 59, 3605 (1999).
[18] S. White, M. Blaskiewicz, W. Fischer, and Y. Luo, ICFA Mini-Workshop on Beam-Beam Effects in Hadron Colliders (BB3013), CERN (2013).
[19] S. Fartoukh, Phys. Rev. ST Accel. Beams 16, 111002 (2013).